A Novel OFDM Scheme for VLC Systems Under LED Nonlinear Constraints

Lingkai Kong, Congcong Cao, Siyuan Zhang, Mengchao Li, Liang Wu(✉), Zaichen Zhang, and Jian Dang

National Mobile Communications Research Laboratory, Southeast University, Nanjing 210096, China
{konglingkai,caocongcong,zhangsiyuan,limengchao,wuliang, zczhang,newwanda}@seu.edu.cn

Abstract. In this paper, a novel optical orthogonal frequency division multiplexing (O-OFDM) scheme based on real-imaginary coefficients separation is proposed for visible light communications (VLCs) to mitigate nonlinear distortion of light-emitting diodes (LEDs). In the proposed scheme, the transmitted signal in the frequency domain does not need to be Hermitian symmetric, and real and imaginary parts are separated. Signals are introduced to keep the clipped information due to the high peak to average power ratio of OFDM, and a procedure to recover the clipped information is proposed. The transmit strategy and receive algorithm of the proposed scheme are presented in detail. Simulation results show that compared with traditional O-OFDM schemes, the proposed scheme can achieve better bit error rate performance under LED nonlinear constraints and reduce the requirement for the linear dynamic range of LEDs.

Keywords: Optical orthogonal frequency division multiplexing (O-OFDM) · Clipped infomation · Coefficients separation · Nonlinear distortion · Light-emitting diodes (LEDs)

1 Introduction

Optical wireless communications which employ light-emitting diodes (LEDs) as transmitters and photodiodes (PDs) as receivers have received increasing attention in both academia and industry due to its inherent high efficiency and security [1]. Intensity modulation and direct detection (IM/DD) is the most commonly used scheme in optical wireless communications [2,3]. In IM/DD systems, the transmitted signals must be nonnegative, and most radio frequency (RF) modulation schemes cannot be directly used.

Recently, orthogonal frequency division multiplexing (OFDM) has been employed in visible light communication (VLC) systems to compat inter-symbol interference (ISI) and achieve high spectral efficiency. To statisfy the requirement in IM/DD system, a number of O-OFDM schemes have been proposed. The simplest method is direct-current biased optical orthogonal frequency division

Q. Chen et al. (Eds.): ChinaCom 2016, Part I, LNICST 209, pp. 393–402, 2018.
DOI: 10.1007/978-3-319-66625-9_38

multiplexing (DCO-OFDM) [4]. Asymmetrically clipped optical OFDM (ACO-OFDM) [5], unipolar OFDM (U-OFDM) [6] and flip OFDM [7] can achieve higher power efficiency than the conventional DCO-OFDM at the expense of losing half of the spectral efficiency. In [8], a real and imaginary coefficients separation OFDM (RIS-OFDM) scheme, which is based on real and imaginary coefficients separation, is proposed in multiple-input multiple-output (MIMO) systems with better performance and lower complexity.

However, there is one common in all of the above schemes that they did not consider the nonlinear distortion by LEDs [9]. By applying a digital predistortion [10], the nonlinear transfer characteristic of LEDs can be modeled as double-side clipping. Unfortunately, the linear region of LEDs is still not large enough in a practical scenario and the nonlinear distortion is still a serious problem which degrades the system performance due to the high peak-to-average-power ratio (PAPR) of O-OFDM. ACO-OFDM specified recoverable upper clipping system is introduced in [11], which fully utilizes the structure of ACO-OFDM to mitigate the nonlinear distortion at the expense of increasing the receiver complexity. Also, its spectral efficiency is low due to the inherent characteristics of ACO-OFDM. In polar OFDM (P-OFDM) [12], a polar coordinate transformation is conducted with abilities to acheive relatively high spectral efficiency and better bit error rate (BER) performance under practical conditions of fixed power and LED nonlinear constraints.

In this paper, we develop a novel O-OFDM system based on real-imaginary coefficients separation and recoverable clipping to mitigate the nonlinear distortion due to LEDs. The proposed system fully utilizes the structure of coefficients separation and dynamic range of LEDs. Simulation results show that the proposed scheme achieves better BER performance under LED nonlinear constraints and reduces the requirement for the linear dynamic range of LEDs compared with DCO-OFDM, ACO-OFDM and P-OFDM.

The rest of the paper is organized as follows. In Sect. 2, the simplified LED nonlinear model is given. The transmit strategy and receive algorithm of the proposed scheme are described in detail in Sect. 3. Then simulation results are presented and discussed in Sect. 4. Finally, Sect. 5 concludes this paper.

2 Nonlinear Model of LED

Because of the p-n junction and the saturation effect of the LEDs, there is a nonlinear relation between the input and the output of the LEDs. However, by applying predistortion techniques [10], The nonlinear transfer characteristic of LEDs can be modeled as double-sided clipping. The simplified LED model in [13] is employed in this paper, and can be expressed as

$$G[x] = \begin{cases} I_L, \ x < I_L \\ x, \quad I_L < x < I_H \\ I_H, x < I_H \end{cases}, \tag{1}$$

where $G\left[\cdot\right]$ denotes the simplified LED nonlinear model, and $[I_L, I_H]$ is the linear region of LED.

To quantify the dynamic range of LEDs, the clipping ratio (CR) is defined as [12]

$$\mathrm{CR}\,(\mathrm{dB}) = 10\log_{10}\frac{I_H - I_L}{P_{\mathrm{opt}}} = 10\log_{10}\frac{DR_{\mathrm{LED}}}{P_{\mathrm{opt}}}, \tag{2}$$

where P_{opt} is the transmitted optical power and DR_{LED} denotes the dynamic range of the LEDs.

3 Proposed O-OFDM Scheme

In this section, a novel O-OFDM system based on real-imaginary coefficients separation and recoverable clipping is proposed to improve BER performance when the linear region of LED is constrained.

3.1 Transmitter

The block diagram of the proposed system is illustrated in Fig. 1. At the transmitter, the modulated information symbols are only mapped onto the odd subcarriers and the even subcarriers are set to zero. Then, the complex data signal in the frequencey domain $\mathbf{X} = [0, X(1), 0, X(3) \cdots, 0, X(N-1)]$ is input into the inverse fast Fourier transform (IFFT) module, where N is the size of IFFT. In contrast to schemes such as ACO-OFDM, $\mathbf{X}$ dose not need to be Hermitian symmetric. After IFFT, the time domain signal $x(n)$ has odd symmetry property, that is

$$x(n) = -x(n + \frac{N}{2});\ n = 0, 1, 2, \cdots, \frac{N}{2} - 1, \tag{3}$$

where $x(n)$ is complex.

Due to the odd symmetry, half of the output signals can be considered as redundant information which can be employed to separate the real and imaginary

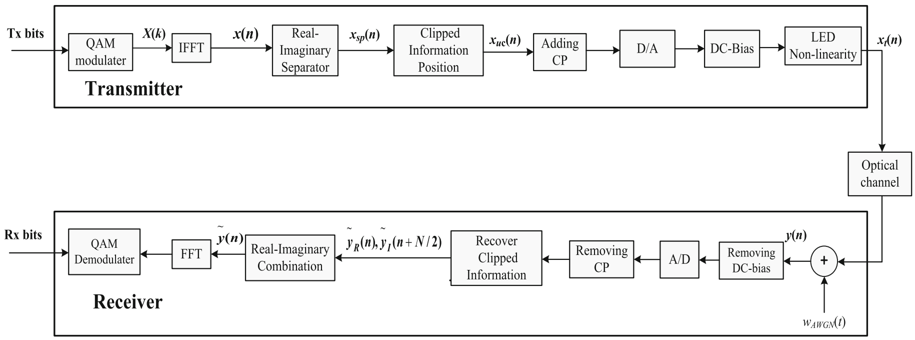

Fig. 1. Block diagram of the proposed system

parts of $x(n) = x_R(n) + jx_I(n)$, where $x_R(n)$ and $x_I(n)$ are real, and the real and imaginary parts of $x(n)$, respectively. The process is described as

$$x_{sp}(n) = \begin{cases} x_R(n), 0 \leq n \leq \frac{N}{2} - 1 \\ x_I(n), \ \frac{N}{2} \leq n \leq N - 1 \end{cases}, \tag{4}$$

where $x_{sp}(n)$ is the n-th time-domain sample after the real-imaginary separator.

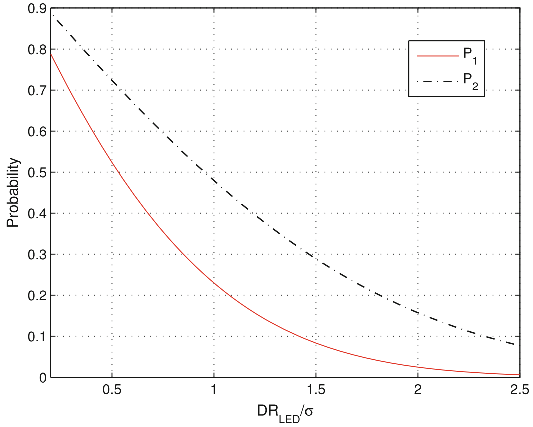

Fig. 2. P_1 and P_2 versus DR_{LED}/σ when $DC = (I_H + I_L)/2$

Although the signals $x_{sp}(n)$ can be transmitted after adding the DC bias, it will suffer severe clipping distortion due to the dynamic range of LEDs. Therefore, we introduce $x_c(n)$ to make the clipped information recoverable. However, if we keep all clipped information, $x_c(n)$ will be as long as $x_{sp}(n)$, which will cost too much. Fortunately, the structure of real-imaginary coefficients separation provides us a better solution. Note that the possibility of $x_R(n)$ and $x_I(n + \frac{N}{2})$ being clipped at the same time follows

$$P_1 = \left(1 - \frac{1}{\sqrt{\pi}\sigma} \int_{I_L - DC}^{I_H - DC} e^{-\frac{x^2}{\sigma^2}} \, dx\right)^2, \tag{5}$$

where σ^2 is the variance of $X(k)$. Figure 2 plots P_1 and P_2 versus DR_{LED}/σ, where DC is set to the middle of the linear range of the LEDs, P_2 denotes the possibility of $x_R(n)$ being clipped, and the possibility of $x_I(n+\frac{N}{2})$ being clipped is equal to P_2. It can be seen that when $DR_{\text{LED}}/\sigma > 2$, the possibility of $x_R(n)$ and $x_I(n+\frac{N}{2})$ being clipped at the same time is smaller than 0.025, which is very small. Therefore, we can just keep one of the clipped information by comparing the absolute value, and the larger one will be kept. To recover the original signal successfully at the receiver, the polarity of $x_c(n)$ will be determined by which part was clipped from, e.g. when it is clipped from $x_R(n)$, $x_c(n)$ will be positive, otherwise, when it is clipped from $x_I(n+\frac{N}{2})$, $x_c(n)$ will be negative. As can be seen that the length of $x_c(n)$ only need to be $\frac{N}{2}$ since the structure of coefficients separation is fully utilized. The recoverable clipping reposition process is illustrated as Fig. 3, which can be mathematically expressed as

$$x_c(n) = \begin{cases} |e_R(n)|, & |e_R(n)| \geq |e_I(n)| \\ -|e_I(n)|, & |e_R(n)| < |e_I(n)| \end{cases}, \tag{6}$$

where $n = 0, 1, 2, \cdots, \frac{N}{2}-1$, $e_R(n)$ and $e_I(n)$ denotes the clipped information of $x_R(n)$ and $x_I(n)$ respectively, which follow

$$e_R(n) = \begin{cases} x_R(n) - \lambda_{\max}, & x_R(n) > \lambda_{\max} \\ 0, & \lambda_{\min} \leq x_R(n) \leq \lambda_{\max} \\ x_R(n) - \lambda_{\min}, & x_R(n) < \lambda_{\min} \end{cases} \tag{7}$$

$$e_I(n) = \begin{cases} x_I(n+\frac{N}{2}) - \lambda_{\max}, & x_I(n+\frac{N}{2}) > \lambda_{\max} \\ 0, & \lambda_{\min} \leq x_I(n+\frac{N}{2}) \leq \lambda_{\max} \\ x_I(n+\frac{N}{2}) - \lambda_{\min}, & x_I(n+\frac{N}{2}) < \lambda_{\min} \end{cases}, \tag{8}$$

where $\lambda_{\max} = I_H - DC$, $\lambda_{\min} = I_L - DC$ and $n = 0, 1, \cdots, \frac{N}{2}-1$. After the recoverable clipping procedure, the signals transmitted by LED can be expressed as

$$x_t(n) = \begin{cases} G[x_{sp}(n) + DC], & 0 \leq n \leq N-1 \\ G[x_c(n-N) + DC]. & N \leq n \leq \frac{3N}{2}-1 \end{cases}. \tag{9}$$

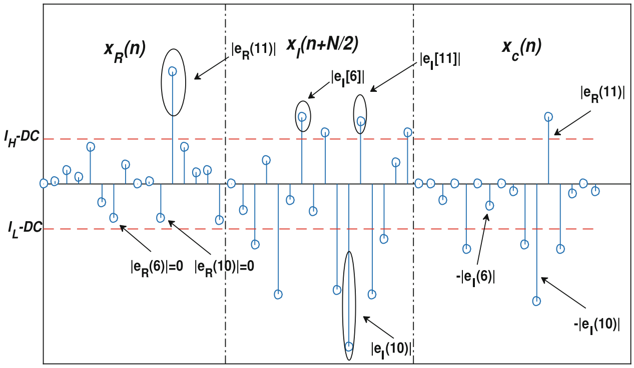

Fig. 3. Example of recoverable clipping procedure

Due to the property of $x_c(n)$, the optical transmitted power of the system do not change and appoximately equals to DC, which is the same as that of DCO-OFDM [14].

3.2 Receiver

Additive white Gaussian noise (AWGN) channel is assumed in this paper, and the received signal $y(n)$ is expressed as

$$y(n) = x_t(n) + w(n), \tag{10}$$

where $w(n)$ is the Gaussian noise component. After removing the DC-bias, define the corresponding received sample group as

$$\gamma(n) = (y_1(n), y_2(n), y_c(n)), \tag{11}$$

where $y_1(n) = y(n) - DC$, $y_2(n) = y(n+\frac{N}{2}) - DC$, $y_c(n) = y(n+N) - DC$ and $n = 0, 1, 2, \cdots, \frac{N}{2} - 1$.

According to $y_c(n)$ and (6), it can be determined where the clipped signal comes from, for example, from $x_R(n)$, or from $x_I(n+\frac{N}{2})$ or neither of them are clipped. Then, whether $y_c(n)$ should be added or subtracted is determined by the polarity of its corresponding part. Therefore, for a given corresponding sample group $\gamma(n)$, there are four decision regions, which can be described as

$$D_1 : \begin{cases} y_c(n) \geq 0, \\ y_1(n) \geq 0; \end{cases} D_3 : \begin{cases} y_c(n) < 0, \\ y_2(n) \geq 0; \end{cases}$$
$$D_2 : \begin{cases} y_c(n) \geq 0, \\ y_1(n) < 0; \end{cases} D_4 : \begin{cases} y_c(n) < 0, \\ y_2(n) < 0. \end{cases} . \tag{12}$$

After the decision region of $\gamma(n)$ has been determined according to (12), the corresponding recovery procedure is

$$(\tilde{y}_R(n), \tilde{y}_I(n+\frac{N}{2})) = \begin{cases} (y_1(n) + y_c(n), y_2(n)), \gamma(n) \in D_1 \\ (y_1(n) - y_c(n), y_2(n)), \gamma(n) \in D_2 \\ (y_1(n), y_2(n) + y_c(n)), \gamma(n) \in D_3 \\ (y_1(n), y_2(n) - y_c(n)), \gamma(n) \in D_4 \end{cases}, \tag{13}$$

where $n = 0, 1, 2, \cdots, \frac{N}{2} - 1$. It should be noted that, due to AWGN, the polarity of $x_c(n)$ may be changed and thus lead to error detection when determining which part it belongs to. However, this situation only happens when $x_c(n)$ is very small or zero thus carrying few clipped information. Therefore, the system performance may not be significantly affected, and the effect is also investigated further in the next section.

Then the real-imaginary combination block will be performed according to (3) and (4), the output is

$$\tilde{y}(n) = \begin{cases} \tilde{y}_R(n) - j\tilde{y}_I(n+\frac{N}{2}), & 0 \leq n \leq \frac{N}{2} - 1 \\ -\tilde{y}(n-\frac{N}{2}), & \frac{N}{2} \leq n \leq N - 1 \end{cases}. \tag{14}$$

After that, the receiver applies FFT, and signals can be demodulated.

The spectral efficiency of the proposed scheme is given by

$$\begin{aligned}\eta_{\text{proposed}} &= \frac{\frac{N}{2}}{N+\frac{N}{2}+N_{\text{cp}}}\log_2(M) \\ &= \frac{N}{3N+2N_{\text{cp}}}\log_2(M),\end{aligned} \tag{15}$$

where M is the modulation order of the modulated subcarriers, and N_{cp} is the length of cyclic prefix (CP). The spectral efficiency of DCO-OFDM is shown as [15]

$$\eta_{\text{DCO-OFDM}} = \frac{N-2}{2(N+N_{\text{cp}})}\log_2(M). \tag{16}$$

Campared with DCO-OFDM, half of the spectral efficiency is lost in ACO-OFDM [14]. Since no Hermitian symmetry is needed in P-OFDM, its spectral efficiency is expressed as [15]

$$\eta_{\text{P-OFDM}} = \frac{N}{2(N+N_{\text{cp}})}\log_2(M). \tag{17}$$

When N is great, we can get

$$\begin{aligned}\eta_{\text{proposed}} &\approx \frac{4}{3}\eta_{\text{ACO-OFDM}} \\ &\approx \frac{2}{3}\eta_{\text{DCO-OFDM}} \approx \frac{2}{3}\eta_{\text{P-OFDM}}.\end{aligned} \tag{18}$$

4 Simulation Results

The performances of the proposed scheme, DCO-OFDM, ACO-OFDM, and P-OFDM are campared in this section. In the simulations, $N = 128$, $P_{\text{elec}} = E[X^2(k)]$ is normalized to 1, and P_{opt} is equal to 30 dBm, i.e. $DC = 1$, to satisfy the illumination requirement. I_L is set to zero. The AWGN channel is considered, and $N_{\text{cp}} = 0$. To achieve the same data rate, 4-QAM is used in DCO-OFDM and P-OFDM, and 8-QAM and 16-QAM are employed in the proposed system and ACO-OFDM, respectively. A scaling factor is used for ACO-OFDM and P-OFDM to achieve the required optical power level [13].

The BER performances of the four O-OFDM scheme are shown in Fig. 4, where CR = 3 dB. At the BER of 10^{-3}, the proposed system achieves significant performance gain of about 5.2 dB and 3.2 dB over DCO-OFDM and P-OFDM, respectively. For ACO-OFDM, it even cannot work under this circumstance because of the severe nonlinear distortion. It can be seen that when SNR is relatively low, the proposed system achieves no performance gain compared with DCO-OFDM, while for high SNR, the proposed system outperforms DCO-OFDM. The reason is that, when SNR is low, the AWGN is the dominant element to affect the system performance instead of nonlinear distortion.

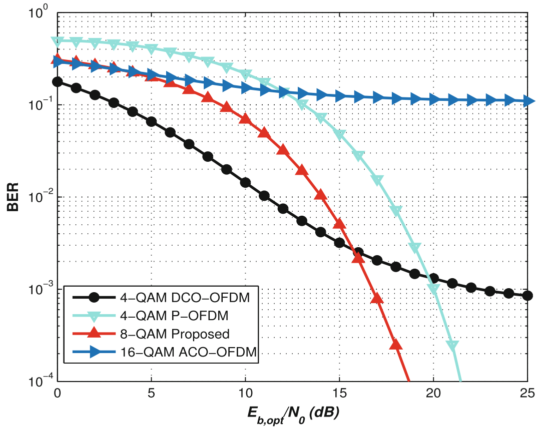

Fig. 4. BER performance comparison among different schemes when CR = 3 dB

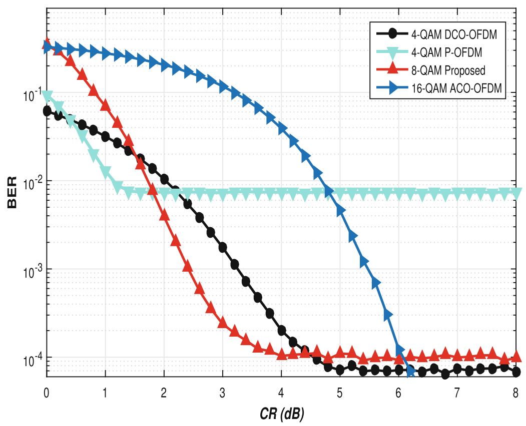

Fig. 5. BER performance versus CR

When SNR increases, which is also the working region for practical systems, the nonlinear distortion is the dominant and the proposed scheme achieves better performance. Besides, there is no error floor in the Proposed scheme.

Figure 5 plots the BER performance of the four schemes versus the CR when $E_{b,\mathrm{opt}}/N_0 = 18$ dB. As shown in Fig. 5, for the proposed scheme, P-OFDM and DCO-OFDM, the BER performance degrades dramatically with the decrease of the CR when the CR is smaller than a threshold due to the insufficient dynamic range. But all of the curves will converge to a BER floor when the CR is large enough. The observed BER floor is mainly determined by the level of the noise. For a target BER of 10^{-3}, the requirement for the CR of the proposed system is approximately 2.4 dB, while that of DCO-OFDM is 3.3 dB. For ACO-OFDM, CR should be greater than 5.5 dB. Therefore, the requirement for CR of the proposed scheme is successfully reduced by 0.9 dB and 3.1 dB compared with DCO-OFDM and ACO-OFDM, respectively. Note that even when CR is large enough, P-OFDM still cannot achieve the target BER in this environment due to the influence of the high noise power. It is also shown that ACO-OFDM is the most susceptible to the impact of the low dynamic range of the LEDs.

It is mentioned that there are two cases when the receiver will detect incorrectly: (1) $x_c(n)$ is zero and thus $y_c(n)$ belongs to neither $y_1(n)$ nor $y_2(n)$; (2) the polarity of $x_c(n)$ is reversed due to the Gaussian noise. A genie detector which always makes the perfect decisions is simulated in Fig. 6, where CR = 3 dB. It is indicated that, with a genie receiver, there would be a 1 dB BER performance gain. Therefore, the proposed scheme can work well, and is not sensitive to the incorectness of the polarity of $x_c(n)$.

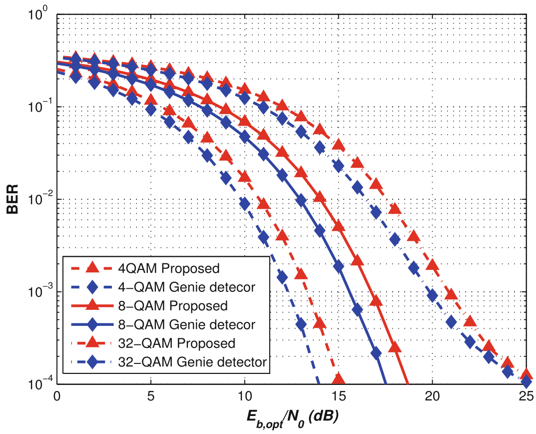

Fig. 6. BER performance comparison with a genie detector under CR = 3 dB

5 Conclusion

A novel O-OFDM scheme based on real-imaginary coefficients separation and recoverable clipping procedure has been proposed in this paper to mitigate the nonlinear distortion due to LEDs. The proposed scheme fully makes use of the structure of coefficients separation and considers the dynamic range of LEDs. In the proposed scheme, the transmitted signal in the frequency domain dose not need to be Hermitian symmetric, and real and imaginary parts of the time domain signal are separated. Compared with DCO-OFDM, ACO-OFDM, and P-OFDM, the proposed scheme can achieve better BER performance under LED nonlinear constraints and reduce the requirement for the linear dynamic range of LEDs The proposed O-OFDM is a promising scheme to be implemented in practical VLC systems.

Acknowledgments. This work is supported by NSFC projects (61501109, 61571105, and 61223001), 863 project (No. 2013AA013601), and Jiangsu NSF project (No. BK20140646).

References

1. Komine, T., Nakagawa, M.: Fundamental analysis for visible-light communication system using LED lights. IEEE Trans. Consum. Electron. **50**(1), 100–107 (2004)
2. Elgala, H., Mesleh, R., Haas, H.: Indoor optical wireless communication: potential and state-of-art. IEEE Commun. Mag. **49**(9), 56–62 (2011)
3. Wu, L., Zhang, Z., Liu, H.: Modulation scheme based on precoder matrix for MIMO optical wireless communication systems. IEEE Commun. Lett. **16**(9), 1516–1519 (2012)
4. Carruthers, J., Kahn, J.: Multiple-subcarrier modulation for nondirected wireless infrared communication. IEEE J. Sel. Areas Commun. **14**(3), 538–546 (1996)
5. Armstrong, J., Lowery, A.J.: Power efficient optical OFDM. Electron. Lett. **42**(6), 370–372 (2006)
6. Tsonev, D., Sinanovic, S., Haas, H.: Novel unipolar orthogonal frequency division multiplexing (U-OFDM) for optical wireless. In: Proceedings of the IEEE 75th Vehicular Technology Conference, p. 15, May 2012
7. Fernando, N., Hong, Y., Viterbo, E.: Flip-OFDM for optical wireless communications. In: Proceedings of the IEEE Information Theory Workshop, p. 59, October 2011
8. Wu, L., Zhang, Z., Liu, H.: Coefficients separation MIMO-OFDM optical wireless communication system in diffuse fading channels. In: Proceedings of the IEEE ICC 2015, London, UK, pp. 5132–5137, June 2015
9. Elgala, H., Mesleh, R., Haas, H.: A study of LED nonlinearity effects on optical wireless transmission using OFDM. In: Proceedings of the WOCN, p. 15, April 2009
10. Dimitrov, S., Haas, H.: Information rate of OFDM-based optical wireless communication systems with nonlinear distortion. J. Lightwave Technol. **31**(6), 918–929 (2013)
11. Xu, W., Wu, M., Zhang, H.: ACO-OFDM-specified recoverable upper clipping with efficient detection for optical wireless communications. IEEE. Photon. **6**(5), 1–17 (2014)
12. Elgala, H., Little, T.D.C.: Polar-based OFDM and SC-FDE links toward energy-efficient Gbps transmission under IM-DD optical system constraints. IEEE/OSA J. Opt. Commun. Netw. **7**(2), A277–284 (2015)
13. Zhang, H., Yuan, Y., Xu, W.: PAPR reduction for DCO-OFDM visible light communications via semidefinite relaxation. IEEE Photon. Technol. Lett. **26**(17), 1718–1721 (2014)
14. Armstrong, J., Schmidt, B.J.C.: Comparison of asymmetrically clipped optical OFDM and DC-biased optical OFDM in AWGN. IEEE Commun. Lett. **12**, 343–345 (2008)
15. Yang, Y., Zeng, Z., Feng, S.: A simple OFDM scheme for VLC systems based on μ-law mapping. IEEE Photon. Technol. Lett. **28**(6), 641–644 (2016)